Reynolds stresses and differential rotation in Boussinesq convection in a rotating spherical shell

Michel Rieutord[1,3], **Axel Brandenburg**[2,3], **André Mangeney**[4], **and Pierre Drossart**[4]

[1] Observatoire Midi-Pyrénées, 14 av. E. Belin, F-31400 Toulouse, France
[2] HAO/NCAR[*], P.O. Box 3000, Boulder, CO 80307, USA
[3] Observatory and Astrophysics Laboratory, P.O. Box 14, SF-00014 University of Helsinki, Finland
[4] Observatoire de Paris-Meudon, F-92195 Meudon Cedex, France

Abstract. We consider the problem of how numerical simulations of convection in a spherical shell can be used to estimate turbulent transport coefficients that may be used in mean field theory. For this purpose we analyse data from simulations of three dimensional Boussinesq convection. The rotational influence on convection is described in terms of the Λ-effect and anisotropic eddy conductivity. When the resulting transport coefficients are used in a mean field model, the original rotation law is recovered approximately. We thus conclude that the flow can be described in terms of a Λ-effect. Our results are also compared with analytical theories and observations.

Key words: hydrodynamics – convection – turbulence – Sun: rotation – stars: rotation

1. Introduction

Understanding the dynamics of stars and giant planets (e.g. differential rotation and magnetic activity) is one of the challenging problems of present day astrophysics. The basic difficulty when dealing with such problems comes from the turbulent nature of the fluid motions in these objects, as no good theory of turbulence yet exists. This lack of understanding leads us to study turbulent flows using experiments. However, in the case of turbulent convection in stars, real experiments are difficult to set up. The main difficulty is to generate the radial gravity. In the experiment of Hart et al. (1986) the radial gravity was simulated by an electric force, and in this way they managed for the first time to simulate convection in a spherical shell. Another convenient way of performing experiments is by using numerical simulations. One solves the set of hydrodynamical equations

and measures, as in experiments, some diagnostic quantities as the flow evolves in time.

We solve the equations of convection for the simple case of a Boussinesq fluid inside a rotating spherical shell. Such a configuration is far from that of a star, but it has frequently been used in the past to investigate the rotational influence on convection in a spherical shell (e.g. Gilman 1977). We concentrate here on determining the turbulent transport coefficients that govern the mean rotation law. Originally, the runs were tailored to represent the outer core of the earth, and that is the reason why we chose the ratio of outer to inner radius to be 0.4, but the results obtained are of more general interest and comparison with the sun can therefore be made.

In the present paper we concentrate on various average properties of the flow and investigate the possibility, of whether these averages can be determined from the simulation and how these functions can be used in mean field models of differential rotation using the Λ-effect approach (Rüdiger 1980). The Λ-effect describes a non-diffusive transport of angular momentum, similarly of the α-effect in mean-field electrodynamics (Krause & Rädler 1980) describes a non-diffusive contribution to the electromagnetic force in addition to the turbulent magnetic diffusion. The Λ-effect is also related to the anisotropic kinetic α-effect (or AKA-effect, Frisch et al. 1987).

In Sect. 2, we describe the basic equations of the problem. We then present results for various averaged quantities (Sect. 3) the Λ-effect (Sect. 4), and the eddy conductivity (Sect. 5). The resulting turbulent transport coefficients are used in a mean field model of differential rotation (Sect 6) and, finally, some astrophysical implications are discussed (Sect. 7).

2. The model

We consider a fluid contained in a spherical shell of outer radius R and inner radius r_0. The fluid is assumed to be incompressible

and the Boussinesq approximation is used. The equation of state is

$$\rho = \rho_0[1 - \alpha(T - T_0)], \qquad (1)$$

where ρ is density, T temperature, α the expansion coefficient and the suffix 0 refers to the hydrostatic reference state. The inner sphere is filled with fluid of the same density but remains at rest. The gravity inside the fluid is

$$g = -\frac{4\pi}{3}G\rho r. \qquad (2)$$

The superadiabatic gradient β is produced by a uniform distribution of heat sources with an energy production rate Q. Such a configuration has often been studied (see e.g. Chandrasekhar 1961; Roberts 1968; Busse & Cuong 1977; Zhang & Busse 1987; Zhang 1992), and its linear stability properties are well known.

Using the thickness d of the shell as the length scale, the dynamical time $t_{\mathrm{dyn}} = (d/\alpha\beta g_0)^{1/2}$ as the time scale (with $g_0 = \frac{4}{3}\pi G\rho d$), and $\beta = Qd^2/3\kappa$ as temperature scale (κ is the heat diffusivity), the nondimensional equations of the fluid motion in a rotating frame of reference are

$$\frac{Du}{Dt} + \mathrm{Fr}\, k \times u = -\nabla P + \Theta x + \sqrt{\frac{\mathscr{P}}{\mathrm{Ra}}}\Delta u, \qquad (3)$$

$$\mathrm{div}\, u = 0, \qquad (4)$$

$$\frac{D\Theta}{Dt} + u \cdot x = \frac{1}{\sqrt{\mathscr{P}\mathrm{Ra}}}\Delta\Theta, \qquad (5)$$

with

$$\mathrm{Fr} = \sqrt{\frac{\mathrm{Ta}\mathscr{P}}{\mathrm{Ra}}}, \quad \mathrm{Ta} = \left(\frac{2\Omega_0 R^2}{\nu}\right)^2, \quad \mathrm{Ra} = \frac{\alpha\beta g_0 d^3}{\nu\kappa}, \qquad (6)$$

where $D/Dt = \partial/\partial t + u \cdot \nabla$ is the total derivative, u the velocity, Θ the temperature fluctuation with respect to the hydrostatic solution, Ω_0 the angular velocity of the initially rigid rotation, ν the kinematic viscosity, k the unit vector in the direction of the rotation axis, x the dimensionless radius vector, $\mathscr{P} = \nu/\kappa$ the Prandtl number, Ra the Rayleigh number, Ta the Taylor number, and Fr is the Froude number. As in the references cited above, we have neglected the centrifugal force and thus the baroclinic flow. The system of equation was completed by stress-free boundary conditions on the velocity on both the inner and outer shell.

Using (4), these equations may be reduced to three scalar equations for the vertical velocity, the vertical vorticity and the temperature fluctuation, which are developed in spherical harmonics for the angular part and Tchebychev polynomials for the radial part, e.g.

$$F(x, \theta, \phi) = \sum_{l,m}^{l_{\max}} \sum_{n}^{n_{\max}} a_{lmn}(t)T_n(x)Y_l^m(\theta, \phi). \qquad (7)$$

The coefficients $a_{lmn}(t)$ are computed using an Adams-Bashforth integration scheme. A Crank-Nicholson scheme is used to treat the diffusion terms implicitly and the other terms explicitly. This same (pseudo-spectral) technique has been used by Glatzmaier & Gilman (1982). The boundary conditions were accounted via a technique proposed by Patera (1984).

Table 1. Parameters of the various runs.

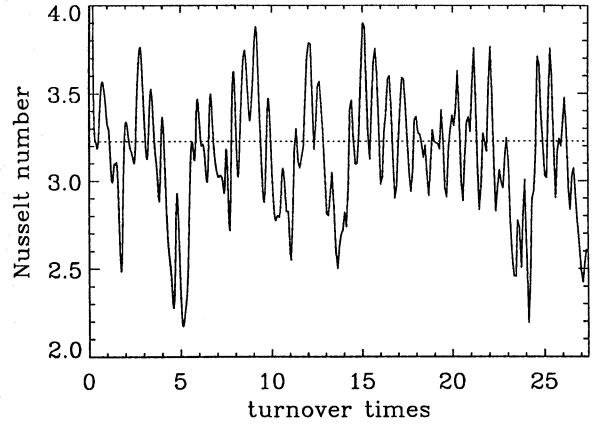|	Run A	Run B	Run C	Run D
Ta	10^5	$1.67\,10^5$	10^6	10^6
Ra	$3.1\,\mathrm{Ra}_c$	$4.4\,\mathrm{Ra}_c$	$4\,\mathrm{Ra}_c$	$8\,\mathrm{Ra}_c$
Nu	3.2	4.2	3.4	8.1
Fr	5.8	5.8	9.5	6.7
u_t	0.65	0.79	0.52	1.0
Ro^{-1}	8.8	7.3	18	6.7

Fig. 1. Time sequence of the Nusselt number (Run A). The abscissa is measures in turnover times. The horizontal, dotted, line indicates the average value

3. Properties of the runs

We accumulated data for runs with different Rayleigh and Taylor numbers. In all cases $\mathscr{P} = 1$, $r_0 = 0.4\,R$, $l_{\max} = 20$ and $n_{\max} = 32$. Conservation of energy and angular momentum was checked in all cases and we confirmed that increasing the resolution did not change the results significantly. The strength of rotation relative to convection is characterised by the inverse Rossby number $\mathrm{Ro}^{-1} = 2\Omega_0 d/u_t$, where u_t is the rms-velocity of the turbulence. The parameters of the runs are summarised in Table 1.

The flow is only mildly supercritical, although many modes are excited and the temporal evolution is irregular (Fig. 1). In this paper we apply this flow to the determination of 'turbulent' transport coefficients, keeping however in mind that the flow is not really turbulent.

In order to facilitate comparison with mean field theory we compute various mean quantities adopting combined longitudinal and temporal averages. For the four runs we present contours of the average angular velocity $\Omega = \Omega_0 + \langle u_\phi\rangle/(r\sin\theta)$, helicity $H = \langle\omega \cdot u\rangle$, where $\omega = \nabla \times u$, and two components of the Reynolds stress tensor, $Q_{r\phi} = \langle u_r'u_\phi'\rangle$ and $Q_{\theta\phi} = \langle u_\theta'u_\phi'\rangle$ (Fig. 2). (Primes denote deviations from the mean.) All four fields are spatially smooth and show almost perfect symmetries about the equator: symmetry for Ω and $Q_{r\phi}$ and antisymmetry for H and $Q_{\theta\phi}$. (In Runs A and C, however, the Rayleigh
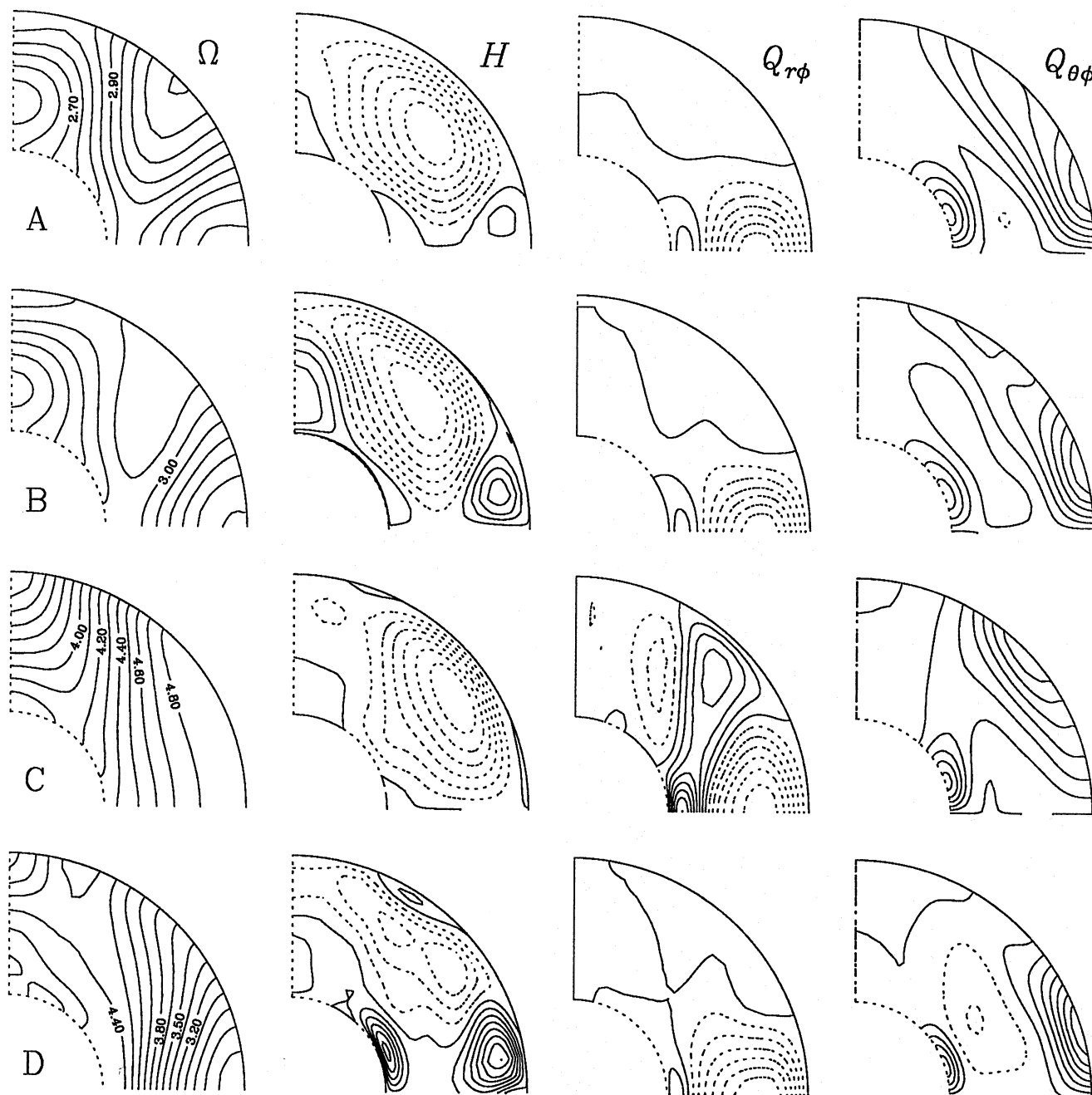
Fig. 2. Contours of angular velocity Ω, helicity H, and two components of the Reynolds stress tensor, $Q_{r\phi}$ and $Q_{\theta\phi}$. Dotted contours refer to negative values

number is still not high enough for antisymmetric modes to be excited.)

In Runs A, B, and D, the angular velocity in the equatorial plane increases toward the centre, whereas in Run C the inverse Rossby number is much larger and the angular velocity now decreases toward the centre. This is in agreement with Gilman (1978) who finds a change from equatorial acceleration to deceleration when (for fixed Taylor number) the Rayleigh number is increased.

The helicity is, as expected, negative (positive) in the northern (southern) hemisphere, but close to the equator near to the surface are 'islands' with opposite helicity. Since at the poles the background vorticity is maximal ($\omega = 2\Omega$), one would also expect there a maximum of H. However, as can be seen from Fig. 3, for large inverse Rossby numbers, the helicity vanishes inside the cylinder tangent to the inner radius of the shell. Consequently, the extrema of the helicity are at mid-latitudes. This is a consequence of the Taylor-Proudman theorem which inhibits vertical motions in polar regions. Thus, the helicity profile is not
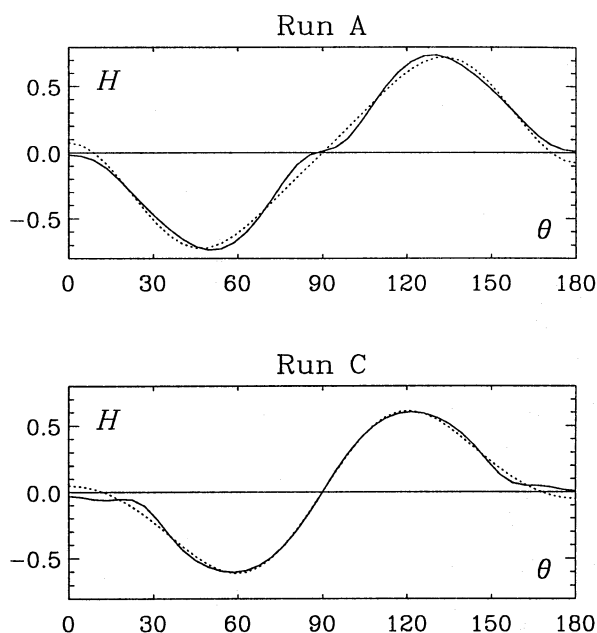
Fig. 3. Latitudinal profile of the helicity at $r = r_m$ (Run A and Run C). The dotted line gives the fit using odd values of ℓ between 1 and 5

Fig. 4. Latitudinal profiles of A_V and A_H, taken in the middle of the layer (Run A)

given by a simple $\cos\theta$ dependence (as one would expect from a simple proportionality to background vorticity) but is better represented by an expression of the form

$$H(r,\theta) = \sum_{\ell=1,3,5,\dots} H_\ell(r) P_\ell(\cos\theta). \tag{8}$$

The coefficients for odd values of ℓ, at mid-depth r_m in the shell are $H_\ell(r_m) = (-0.7, +0.6, +0.2)$ (for Run A), $(-0.9, +0.6, +0.5)$ (for Run B), $(-0.6, +0.7, -0.1)$ (for Run C), and $(-0.5, +0.3, -0.5)$ (for Run D). The profile of $H(r_m)$ and its fit for Run A are plotted in Fig. 3.

The helicity is related to the α-effect in mean field dynamo theory. An expansion similar to Eq. (8) has been obtained for the α-effect (cf. Schmitt 1987). This has important consequences for constructing solar dynamo models, because the correct field geometry can only be reproduced if α decreases toward higher latitudes (e.g. Yoshimura 1975; Belvedere et al. 1991).

In the following we are interested in the Λ-effect, which only exists if the flow is anisotropic. It is therefore important to characterise the degree of anisotropy of the flow. Following Rüdiger (1980), we define

$$A_V = (\langle u_\phi^2 \rangle - \langle u_r^2 \rangle)/u_t^2, \quad A_H = (\langle u_\phi^2 \rangle - \langle u_\theta^2 \rangle)/u_t^2, \tag{9}$$

that describe the anisotropy in the vertical and horizontal directions. In Fig. 4 we plot A_V and A_H as a function of latitude for the middle of the layer. Note that A_V is negative at low latitudes, and positive at higher latitudes. Since the sign of A_V determines the radial gradient of Ω (Rüdiger 1980), we expect that at low latitudes Ω increases inwards, but outwards at higher latitudes (for Run A). This is in agreement with the differential rotation obtained in the simulation.

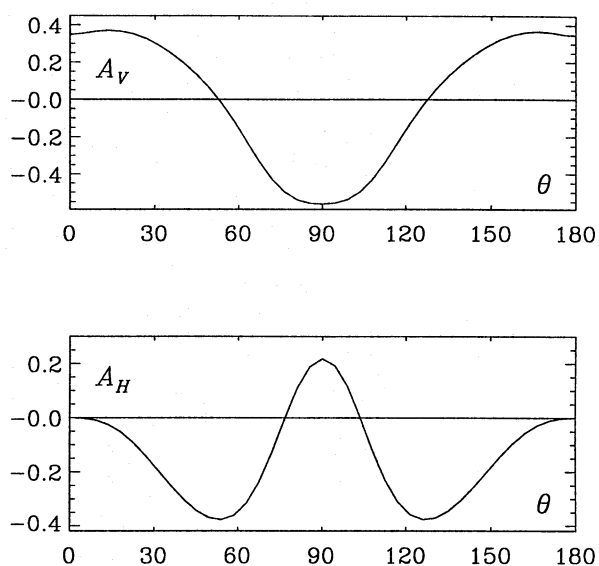## 4. The Λ-effect

The flows presented in this paper display differential rotation as a natural consequence of the rotational effects on the turbulence. In the context of solar and stellar convection zones this mean flow may be described by the Λ-effect (Rüdiger 1980, 1989; Kitchatinov 1986; Durney 1987, 1991). Clearly, our simulations cannot reach the extreme parameter regime relevant to solar convection, but it is nevertheless possible to verify the concept of the Λ-effect and to determine the governing parameters. For this purpose, we compute the components of the Reynolds stress and try to express them in terms of the mean velocity and its gradients. Since in our cases the dominant component of velocity is the azimuthal one, we restrict the dependence of the Reynolds stress to this component. In this connection, we develop a general formalism that may readily be applied to other convection simulations in spherical geometry.

4.1. The horizontal part of the Λ-effect

We consider first the horizontal part of the Λ-effect which is important, because of the observational evidence (Ward 1965; Gilman 1984; Virtanen 1989; Tuominen 1990).

The horizontal component of the Reynolds stress tensor, $Q_{\theta\phi}$, may be written in the form

$$Q_{\theta\phi} = \cos\theta \Lambda_H \Omega - \nu_t^{(H)} \sin\theta \frac{\partial\Omega}{\partial\theta}, \tag{10}$$

where Λ_H is usually written as

$$\Lambda_H = \nu_t[H^{(1)}\sin^2\theta + H^{(2)}\sin^4\theta] \tag{11}$$

(Rüdiger 1980). Here, we have distinguished between the isotropic turbulent viscosity ν_t and a horizontal part $\nu_t^{(H)}$. The coefficient $H^{(1)}$ has been derived from the Greenwich sunspot

data (Ward 1965; Gilman 1984). More recently, Virtanen (1989) and Tuominen (1990) repeated this analysis and determined also $H^{(2)}$. In those studies the representation

$$Q_{\theta\phi} = \nu_t \Omega_0 \cos\theta \sin^2\theta (w_1 + w_2 \sin^2\theta) \quad (12)$$

has been used, where the solar rotation law is already incorporated, and $\nu_t^{(H)} = \nu_t$ is assumed. The analysis of Virtanen (1989) and Tuominen (1990) gives $w_1 = 1$ and $w_2 = 5.6$. Ward (1965) determined also one of the coefficient, namely $w_1 = 2$ (see Rüdiger 1989); however, since the expansion in term of $\sin^2\theta$ is not an orthogonal one, two representations with different order of truncation are not directly comparable. Ward used only one coefficient, thus its value cannot be compared to the others mentioned in the text. The coefficients w_1 and w_2 have also been derived from numerical simulations of rotating turbulent convection in a box located at different latitudes (Pulkkinen et al. 1991, 1993), who finds $w_1 = 1$ and $w_2 = 5$.

We now expand Ω, $Q_{\theta\phi}$, and Λ_H in terms of orthogonal functions

$$\Omega = \frac{1}{\sin\theta} \sum_{k=1,3,5} \omega_k P_k^1(\cos\theta), \quad (13)$$

$$Q_{\theta\phi} = \sum_{n=3,5,7} q_n^{(H)} P_n^2(\cos\theta), \quad (14)$$

$$\cos\theta \Lambda_H = \nu_t \sin\theta \sum_{\ell=2,4,6} \lambda_\ell^{(H)} P_\ell^1(\cos\theta), \quad (15)$$

where we have assumed symmetry about the equator which, in our case, is indeed a good approximation (even for Run B where antisymmetric modes were excited, symmetric modes imposed their symmetry; see Fig. 2). Note also that we restricted ourselves to the first three terms in this expansion. The coefficients ω_k, $q_n^{(H)}$, $\lambda_\ell^{(H)}$, and $\nu_t^{(H)}$ are functions of depth, but we focus attention to their values at the surface, where $Q_{\theta\phi}$ is larger than inside the shell, and where comparisons with observations are possible. (Note that we use a definition for the associated Legendre polynomials, which have a minus sign for odd m-values, e.g. $P_1^1(\cos\theta) = -\sin\theta$). For comparison purposes, we also give the expressions of $H^{(1)}$ and $H^{(2)}$ in terms of $\lambda_\ell^{(H)}$:

$$H^{(1)} = -3\lambda_2^{(H)} - 10\lambda_4^{(H)}, \qquad H^{(2)} = 35/2 \lambda_4^{(H)} \quad (16)$$

The coefficients ω_ℓ and $q_\ell^{(H)}$ are obtained by fitting (13) and (14) to the profiles of Ω and $Q_{\theta\phi}$ as measured from simulations or observations. Inserting (13)–(15) into Eq. (10), multiplying by $P_n^2(\cos\theta)$, and integrating over the sphere we find

$$q_n^{(H)} = \sum_{k=1,3,5} \sum_{\ell=2,4,6} F_{k\ell n} \omega_k \lambda_\ell^{(H)} - \nu_t^{(H)} \omega_n \quad n = 3,5,7. \quad (17)$$

The coupling coefficients

$$F_{k\ell n} = \int P_k^1 P_\ell^1 P_n^2 dz \Big/ \int P_n^2 P_n^2 dz \quad (18)$$

can be expressed in terms of Gaunt integrals or Clebsch-Gordon coefficients, and the relevant ones are given in Table 2.

The system of Eq. (17) is underdetermined, because we have 3 equations and 4 unknowns (the three $\lambda_\ell^{(H)}$ and $\nu_t^{(H)}$). We therefore consider different approaches. In principle, $\nu_t^{(H)}$ can be estimated by

$$\nu_t = \tfrac{1}{3} u_t \ell, \quad (19)$$

where ℓ is the correlation length of the turbulence. Following Pulkkinen et al. (1993), we set $\ell = d$ and assume $\nu_t^{(H)} = \nu_t$ and solve for the three $\lambda_\ell^{(H)}$. On the other hand, we may omit $\lambda_6^{(H)}$ in the expansion (15) and solve explicitly for $\nu_t^{(H)}$ together with the first two $\lambda_\ell^{(H)}$-coefficients. In the first case we solve

$$\nu_t A_{\alpha\beta}^{(H)} \lambda_{2\beta}^{(H)} = q_\alpha^{(H)} + \nu_t \omega_{2\alpha+1}, \quad \alpha,\beta = 1,2,3, \quad (20)$$

and in the second

$$\nu_t A_{\alpha\beta}^{(H)} L_\beta^{(H)} = q_\alpha^{(H)}, \quad \alpha,\beta = 1,2,3, \quad (21)$$

where $L^{(H)} = (\lambda_2^{(H)}, \lambda_4^{(H)}, \nu_t^{(H)})$ is a vector and

$$A_{\alpha\beta}^{(H)} = \left[(1 - \delta_{\beta3}) \sum_{k=1,3,5} F_{k,2\beta,2\alpha+1} \omega_k \right] - \delta_{\beta3} \omega_{2\alpha+1} \quad (22)$$

is a 3×3 matrix where $\omega_7 = 0$ is assumed. In components, Eq. (21) reads

$$\begin{pmatrix} F_{k,2,3}\omega_k & F_{k,4,3}\omega_k & -\omega_3 \\ F_{k,2,5}\omega_k & F_{k,4,5}\omega_k & -\omega_5 \\ F_{k,2,7}\omega_k & F_{k,4,7}\omega_k & 0 \end{pmatrix} \begin{pmatrix} \lambda_2^{(H)} \\ \lambda_2^{(H)} \\ \nu_t^{(H)} \end{pmatrix} = \begin{pmatrix} q_3^{(H)} \\ q_5^{(H)} \\ q_7^{(H)} \end{pmatrix}, \quad (23)$$

where summation over k is assumed.

In Table 3 we give the results for $\lambda^{(H)}$ for three different cases: (i) $\nu_t^{(H)}$ is solved for, (ii) $\nu_t^{(H)} = 0$ is assumed, and (iii) $\nu_t^{(H)} = \nu_t$ is assumed. The results for other values of $\nu_t^{(H)}$ can be obtained by linear interpolation between the cases (ii) and (iii). Mean field theory predicts that the λ-coefficients are quenched with increasing rotation rate (Kitchatinov & Rüdiger 1993). Some of the $\lambda^{(H)}$-coefficients in Table 3 do indeed seem to vary systematically with the inverse Rossby number, although these coefficients may still change sign within the range of Rossby numbers considered.

For Run A the surface rotation law and the $Q_{\theta\phi}$ component are plotted in Fig. 5 together with the fits (13)-(15). The results for the various coefficients are summarised in Table 3. The w_ℓ-coefficients in (12) are related to the $q_\ell^{(H)}$-coefficients. For Run A, for example, we find $w_2/w_1 \approx 3.5$, which is a similar ratio to that given by Virtanen (1989) and Pulkkinen et al. (1993). The $\lambda_\ell^{(H)}$-coefficients corresponding to the w_ℓ-coefficients measured for the sun are $\lambda_2^{(H)} = -1.4$ and $\lambda_4^{(H)} = +0.2$, i.e. $\lambda_4^{(H)}/\lambda_2^{(H)} = -0.14$. In the case where $\nu^{(H)}$ is given, the resulting $\lambda_\ell^{(H)}$-coefficients depend linearly on $\nu^{(H)}$. Thus, $\lambda_4^{(H)}/\lambda_2^{(H)} = -0.14$ could be reproduced by taking a relatively small value of $\nu^{(H)}$. On the other hand, if we solve directly

Table 2. Coefficients $F_{k\ell n} = \int P_k^1 P_\ell^1 P_n^2 dz / \int P_n^2 P_n^2 dz$

n	3			5			7		
$k \backslash \ell$	2	4	6	2	4	6	2	4	6
1	1/5	−1/9	0	0	1/9	−1/13	0	0	1/13
3	1/5	8/33	−35/143	1/7	32/273	1/13	0	50/429	177/2431
5	−2/11	125/429	49/143	1/13	5/39	32/221	15/143	625/7293	4050/46189
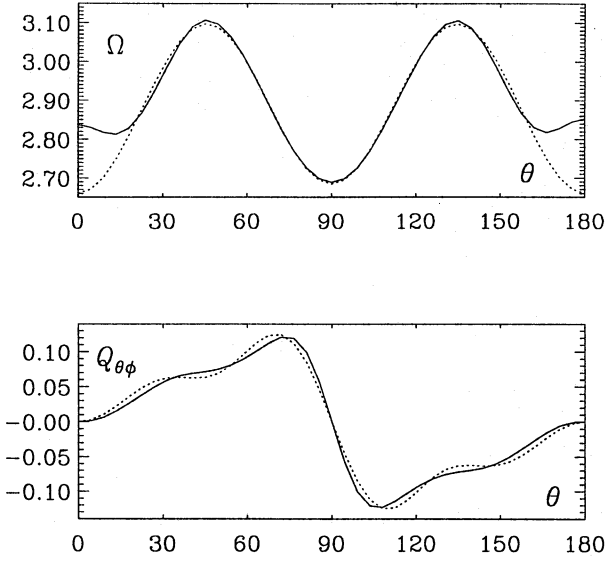
Fig. 5. The surface rotation law for Run A and the horizontal component $Q_{\theta\phi}$ of the Reynolds stress tensor (solid lines) together with the fits (13) and (15) (dotted lines)

for $\nu^{(H)}$ then we get unrealistically large values, and in deeper layers $\nu^{(H)}$ can even become negative. This is clearly an artifact of our method being too sensitive to small changes in the gradient of Ω.

Note that $Q_{\theta\phi}$ is positive in the northern hemisphere. This is an important result, because it shows that Eq. (10) cannot be satisfied without the Λ_H term, provided $\nu_t^{(H)} > 0$. Rüdiger (1977) applied this argument to the sun where $Q_{\theta\phi} > 0$ (from sunspot proper motions) and $\partial\Omega/\partial\theta > 0$ in the northern hemisphere.

4.2. The vertical part of the Λ-effect

We now consider the vertical part of the Λ-effect. Following Rüdiger (1980), the vertical component, $Q_{r\phi}$, of the Reynolds stress tensor is expressed in the form

$$Q_{r\phi} = \sin\theta\Lambda_V\Omega - \nu_t^{(V)}\sin\theta\,\partial\Omega/\partial\ln r, \tag{24}$$

where Λ_V is written as

$$\Lambda_V = \nu_t[V^{(0)} + V^{(1)}\sin^2\theta + V^{(2)}\sin^4\theta]. \tag{25}$$

Again, we expand $Q_{r\phi}$ and Λ_V in terms of orthogonal functions

$$Q_{r\phi} = \sum_{n=1,3,5} q_n^{(V)} P_n^1(\cos\theta), \tag{26}$$

Table 3. The coefficients for the horizontal Λ-effect at $r = R$. The root-mean-square deviation from the fits is around 16%. The three columns for $\lambda^{(H)}$ are for the cases where $\nu_t^{(H)}$ is solved (i), taken to be zero (ii), and assumed to be given by ν_t (iii)

	n	ω_{2n-1}	$q_{2n+1}^{(H)}$	$\lambda_{2n}^{(H)}$ (i)	(ii)	(iii)
A	1	−2.874	0.01909	0.31	−0.142	−0.091
	2	−0.072	−0.00237	−1.15	0.014	−0.119
	3	0.043	0.00149	$(8.8\nu_t)$	−0.034	−0.030
B	1	−2.806	0.02499	0.53	−0.145	−0.005
	2	−0.136	−0.00607	−0.82	0.038	−0.139
	3	0.057	0.00319	$(4.8\nu_t)$	−0.061	−0.048
C	1	−4.830	0.01228	−0.22	−0.077	−0.162
	2	0.037	0.00061	−0.14	−0.005	−0.087
	3	0.041	−0.00035	$(1.6\nu_t)$	0.005	0.002
D	1	−3.033	0.02134	1.33	−0.077	0.319
	2	−0.290	−0.01069	−0.28	0.061	−0.036
	3	0.024	0.00414	$(3.6\nu_t)$	−0.057	−0.041

$$\Lambda_V = \nu_t \sum_{\ell=0,2,4} \lambda_\ell^{(V)} P_\ell(\cos\theta). \tag{27}$$

The relations between the $\lambda_\ell^{(V)}$ and the $V^{(n)}$ are:

$$V^{(0)} = \lambda_0^{(V)} + \lambda_2^{(V)} + \lambda_4^{(V)} \tag{28}$$

$$V^{(1)} = -3/2\lambda_2^{(V)} - 5\lambda_4^{(V)}, \qquad V^{(2)} = 35/8\lambda_4^{(V)} \tag{29}$$

The coefficients $q_n^{(V)}$ can be obtained by fitting (14) to the profile of $Q_{r\phi}$. Inserting (13), (26) and (27) into Eq. (24), multiplying by $P_n(\cos\theta)$, and integrating over the sphere, we find

$$q_n^{(V)} = \sum_{k=1,3,5}\sum_{\ell=0,2,4} G_{k\ell n}\omega_k'\lambda_\ell^{(V)} - \nu_t^{(V)}\omega_n'. \tag{30}$$

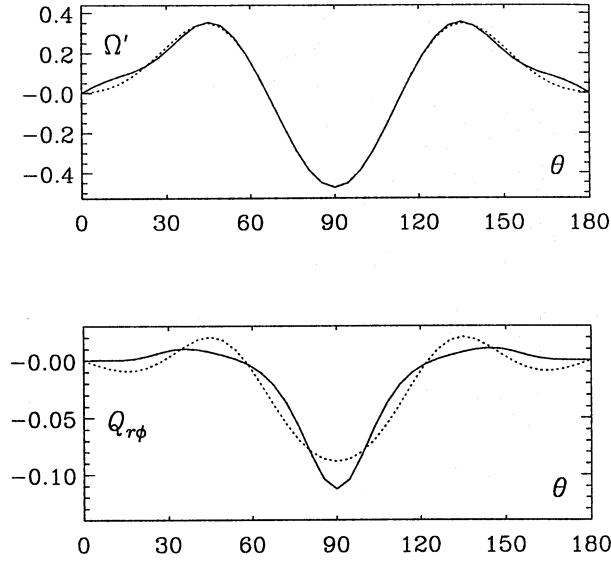where $\omega_k' = \partial\omega_k/\partial\ln r$, and the coefficients

$$G_{k\ell n} = \int P_k^1 P_\ell P_n^1 dz \left/ \int P_n^1 P_n^1 dz \right. \tag{31}$$

are given in Table 4.

Similarly as for the horizontal Λ-effect we either set $\nu_t^{(V)} = \nu_t$, or we omit $\lambda_4^{(V)}$ in the expansion (27) and solve for $\nu_t^{(V)}$

Table 4. Coefficients $G_{k\ell n} = \int P_k^1 P_\ell^1 P_n^1 dz / \int P_n^1 P_n^1 dz$

n	1			3			5		
$k\backslash\ell$	0	2	4	0	2	4	0	2	4
1	1	$-1/5$	0	0	1/5	$-1/9$	0	0	1/9
3	0	18/35	$-2/7$	1	1/5	1/33	0	2/7	22/273
5	0	0	5/11	0	5/11	5/39	1	3/13	4/39

Fig. 6. The profiles of $\Omega' \equiv \partial\Omega/\partial \ln r$ and $Q_{r\phi}$ for Run A (solid lines) together with the fits (13) and (27) (dotted lines)

explicitly. In the second case we obtain $\lambda_0^{(V)}$, $\lambda_4^{(V)}$, and $\nu_t^{(V)}$ by solving the following system of linear equations

$$\nu_t A_{\alpha\beta}^{(V)} L_\beta^{(V)} = q_\alpha^{(V)}, \quad \alpha, \beta = 1, 2, 3, \tag{32}$$

where $L = (\lambda_0^{(V)}, \lambda_2^{(V)}, \nu_t^{(V)})$ is a vector and

$$A_{\alpha\beta} = \left[(1 - \delta_{\alpha 3}) \sum_{k=1,3,5} G_{k,2\beta-2,2\alpha-1} \omega_k \right] - \delta_{\alpha 3} \omega'_{2\alpha-1} \tag{33}$$

is a 3×3 matrix. The result is shown in Fig. 6 and Table 5. Note that the convergence of the $q_\ell^{(V)}$ is much slower than that of $q_\ell^{(H)}$. If we solve for $\nu_t^{(V)}$, we always find negative values. This is an artifact of our method (see the discussion in the previous subsection). Note also that Table 5 shows a systematic dependence of some of the $\lambda^{(V)}$ coefficients on the inverse Rossby number, similarly as for $\lambda^{(H)}$.

4.3. The meridional part of the Reynolds stress tensor

The theory of the meridional part of the Reynolds stress tensor is not well developed, mostly because it does not occur in the equation for the angular velocity. Although this term is not directly important for driving differential rotation, it does occur in

Table 5. The coefficients for the vertical Λ-effect at $r = r_m$. The root-mean-square deviation from the fits is around 26%. The three columns for $\lambda^{(V)}$ are for the cases where $\nu_t^{(V)}$ is solved (i), taken to be zero (ii), and assumed to be given by ν_t (iii)

	n	ω_{2n-1}	ω'_{2n-1}	$q_{2n-1}^{(V)}$	$\lambda_{2n-2}^{(V)}$ (i)	(ii)	(iii)
A	1	-2.886	0.05	0.040	-0.063	-0.05	-0.02
	2	-0.028	-0.20	-0.02	-0.06	0.10	0.32
	3	0.042	0.07	0.010	$(-0.7\nu_t)$	-0.15	-0.36
B	1	-2.976	0.54	0.060	0.002	-0.06	-0.17
	2	-0.057	-0.34	-0.03	-0.15	0.10	0.52
	3	0.059	0.09	0.014	$(-0.6\nu_t)$	-0.17	-0.47
C	1	-4.631	-0.87	0.006	-0.087	-0.01	0.16
	2	0.083	0.02	0.00	0.03	-0.01	-0.09
	3	0.027	0.07	0.005	$(-0.4\nu_t)$	-0.06	-0.19
D	1	-3.723	2.44	0.072	0.239	-0.05	-0.58
	2	-0.212	-0.52	-0.03	-0.33	0.06	0.78
	3	0.051	0.02	0.013	$(-0.5\nu_t)$	-0.11	-0.30

the meridional part of the momentum equation and might be responsible for modifying and, perhaps, reducing the meridional flow that is generated from the differential rotation. Thus, since a meridional flow can modify the rotation law, the meridional part of the Reynolds stress tensor can indirectly be important.

For rapid rotation Q_{ij} has, in addition to the diffusive part, a component proportional to $\Omega_i\Omega_j$. In the following we focus on the (r, θ)-component, which is proportional to $-\sin\theta\cos\theta$, and write

$$Q_{r\theta} = \sin\theta\cos\theta\Lambda^{(M)} - D_{r\theta}, \tag{34}$$

where

$$D_{r\theta} = \nu_t \left[\frac{1}{r}\frac{\partial u_r}{\partial\theta} + r\frac{\partial}{\partial r}\left(\frac{u_\theta}{r}\right) \right] \tag{35}$$

is the diffusive term. We expand $\Lambda^{(M)}$ as

$$\sin\theta\cos\theta\Lambda^{(M)} = (\nu_t\tau_{\text{corr}}\Omega^2) \sum_{\ell=2,4,6} q_\ell^{(M)} P_\ell^1(\cos\theta) \tag{36}$$

In Fig. 7 we plot $Q_{r\theta}$, $D_{r\theta}$, and $Q_{r\theta}^{(M)} \equiv Q_{r\theta} + D_{r\theta}$ at $r = r_m$. The expansion coefficients for Run A are

$$q_2^{(M)} = 0.021, \quad q_4^{(M)} = 0.007, \quad q_6^{(M)} = -0.010. \tag{37}$$

For comparison with the results of Pulkkinen et al. (1993) it is useful to write $Q_{r\theta}^{(M)}$ in the form $\Lambda_M = M^{(1)} + M^{(2)} \sin^2\theta$). We find $M^{(1)} = -0.14$ and $M^{(2)} = 0.13$, whereas Pulkkinen et al. find $M^{(1)} = -0.03$ and $M^{(2)} = 0.06$.

5. The eddy conductivity

We now consider the eddy conductivity that relates the convective flux $\langle u'T' \rangle$ to the average temperature gradient via

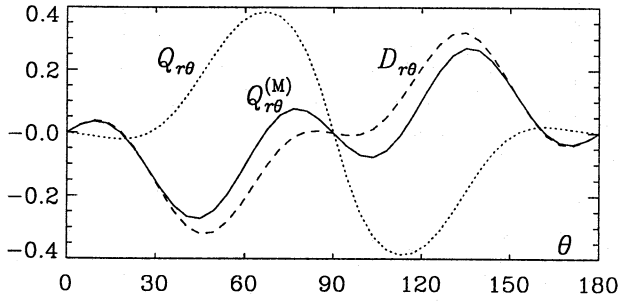$$\langle u_i'T' \rangle = -\chi_{ij}\nabla_j\langle T \rangle. \tag{38}$$

Fig. 7. The profiles of $Q_{r\theta}$ (dotted), $D_{r\theta}$ (dashed), and $Q_{r\theta}^{(M)} \equiv Q_{r\theta} + D_{r\theta}$ (solid line) at mid-radius (Run A)

Since we adopt longitudinal averages, the ϕ-component of $\nabla \langle T \rangle$ vanishes. Furthermore, since the θ-component of $\nabla \langle T \rangle$ is small, we restrict ourselves only to the r-component of $\nabla \langle T \rangle$, and consequently only to the χ_{rr} and $\chi_{\theta r}$ components of the eddy conductivity tensor. Following Rüdiger (1980), χ_{rr} and $\chi_{\theta r}$ are expressed in the form

$$\chi_{rr} = \chi_t \left(VV^{(0)} - VV^{(1)} \sin^2 \theta - VV^{(2)} \sin^4 \theta \right), \tag{39}$$

$$\chi_{\theta r} = -\chi_t \left(HV^{(1)} + HV^{(2)} \sin^2 \theta \right) \sin \theta \cos \theta, \tag{40}$$

where we put $\chi_t = \nu_t$. We expand χ_{rr} and $\chi_{\theta r}$ in terms of orthogonal functions

$$\chi_{rr} = \chi_t \sum_{n=0,2,4} \chi_\ell^{(V)} P_\ell(\cos \theta), \tag{41}$$

$$\chi_{\theta r} = \chi_t \sum_{n=2,4,6} \chi_\ell^{(H)} P_\ell^1(\cos \theta). \tag{42}$$

The profiles of χ_{rr} and $\chi_{\theta r}$ are given in Fig. 8 together with the fits (41) and (42). The diffusion in the radial direction is larger close to the equator than at the poles. This may be explained by the Taylor-Proudman theorem which inhibits large scale motions along the rotation axis: heat transport is then reduced. This point was also noticed by Pulkkinen et al. (1993): when the latitude of their computational domain increased, the critical Rayleigh number increased as well. Note that mean field theory predicts (Kitchatinov et al. 1993) that in the limit of rapid rotation, diffusion is strongest in the direction of the rotation axis. This contradiction is connected to the assumption of a peaked power spectrum, which is assumed in that theory (cf. Rüdiger 1989) and which does not apply in our simulations. Another reason for the difference may be related to the fact that in mean field theory the correlation lengths along the axis is enhanced, and therefore the turbulent diffusion in this direction increased. In our simulations, however, the flow is not sufficiently turbulent and therefore the correlation length is always comparable to the thickness of the convective shell.

If the isotropic part of χ is associated with $\chi_t \chi_0^V$, we find values between 0.2 and 0.7 (Table 6), indicating that χ_t is somewhat smaller than $\frac{1}{3} u_t \ell$.
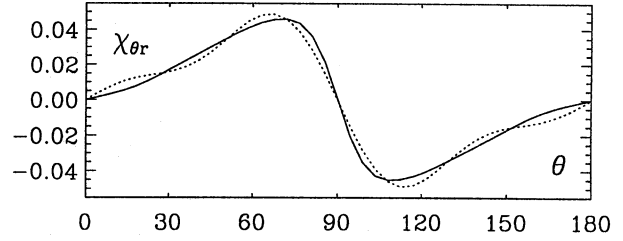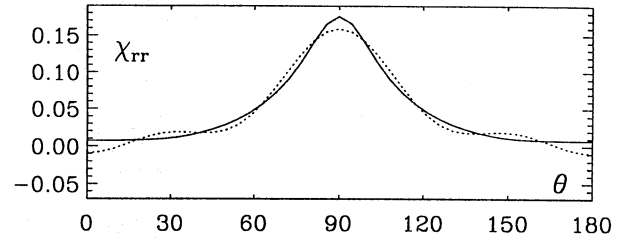

Fig. 8. The profiles of χ_{rr} and $\chi_{\theta r}$ at mid-radius (Run A)

Table 6. The coefficients for the eddy conductivity tensor. The root mean square deviation of the fits is 13% for Run A, 22% for Run B, 5% for Run C, and 40% for Run D

	n	χ_{2n-2}^V	χ_{2n}^H	$VV^{(n-1)}$	$HV^{(n-1)}$
A	1	0.3085	−0.1239	0.1508	
	2	−0.4856	0.0435	−0.9111	−0.0636
	3	0.3279	−0.0147	1.4345	0.7618
B	1	0.3875	−0.1151	0.2614	
	2	−0.6264	0.0347	−1.5617	−0.0016
	3	0.5003	−0.0141	2.1886	0.6072
C	1	0.2006	−0.0413	0.0400	
	2	−0.2900	0.0182	−0.2120	−0.0578
	3	0.1294	−0.0040	0.5661	0.3179
D	1	0.6624	−0.0882	0.7145	
	2	−1.3010	0.0373	−4.8139	−0.1086
	3	1.3531	−0.0117	5.9197	0.6528

6. Application to mean field models

Having obtained the coefficients of the Λ-effect, we can use them in a mean field model of differential rotation. It is important to include the depth dependence of those coefficients in the model. In Fig. 9 we show $\lambda_\ell^{(V)}$ and $\lambda_\ell^{(H)}$ as a function of depth. For comparison, the corresponding surface values of $H^{(1)}$ and $H^{(2)}$ are +0.10 and +0.07. At the surface, the V-coefficients vanish, but for example at the mid-radius of the shell be have $V^{(0)} = -0.03$, $V^{(1)} = +0.18$, $V^{(2)} = -0.20$.

We use these coefficients to compute a model of differential rotation assuming a uniform turbulent viscosity ν_t with a *turbulent* Taylor number of 10^4 (for details of the method see Brandenburg et al. 1992). The resulting contours of the differential rotation and the surface rotation law are plotted in Fig. 10. There is clear, but no perfect, agreement between the original rotation law and that inferred from the Λ-effect coefficients.
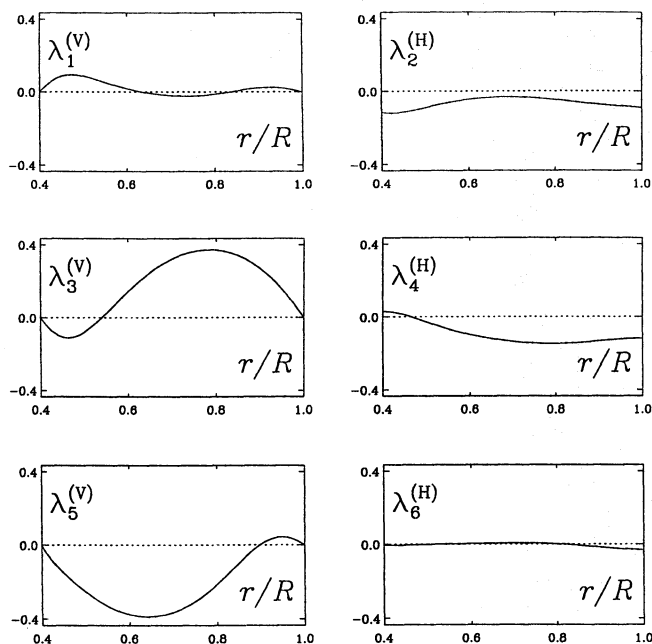
Fig. 9. Depth dependence of $\lambda_\ell^{(V)}$ (left) and $\lambda_\ell^{(H)}$ (right) for Run A
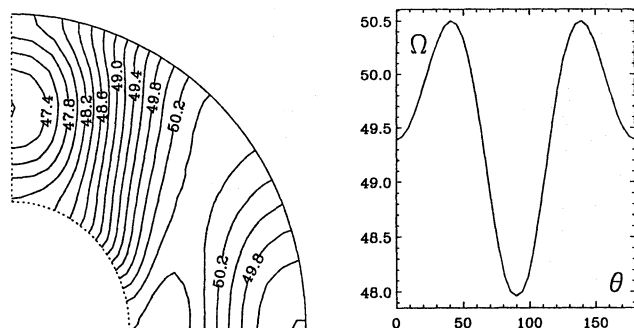

Fig. 10. Contours of differential rotation and surface rotation law for a mean field model using the coefficients of the Λ-effect determined above from Run A. (Ω is measured in units of ν_t/R^2.) Note the similarity with the original rotation law (see Figs. 2 and 5)

Thus, a description in terms of mean field theory seems to be possible, even though the fluid is not really turbulent.

7. Discussion

We have developed tools for estimating turbulent transport coefficients from convection simulations in a spherical shell. Here we only applied these tools to incompressible simulations of small Rayleigh number and it would be important to investigate the trends as more realistic parameter regimes are approached. However, even though our simulations are rather idealised, they do show the existence of the Λ-effect: without the Λ-effect it would be impossible to explain the positiveness of the $Q_{\theta\phi}$ component of the Reynolds stress.

Note that we have omitted the anisotropy of the turbulent viscosity, because it is not the primary driver for differential ro-

tation. However, in real applications this needs to be included. Like all diffusive turbulent transport effects, such terms are difficult to determine, because they multiply average gradients that are often small and therefore not very accurately determined, which leads to uncertain results. More direct methods for determining such diffusive transport coefficients therefore need to be developed.

It is remarkable that the latitudinal distribution of the helicity and various Reynolds stress components can be rather complicated, and the convergence of the expansions can be rather slow. This is partly because of moderate and rapid rotation that generally leads to the occurrence of higher order terms. In the models presented here the inverse Rossby number does exceed unity, and this is typical for the sun. It is therefore conceivable that some of the trends shown here may also be found in the sun. The helicity decreases towards the poles and close to the surface and at the bottom it may even change sign at mid-latitudes. This has important implications for mean field dynamo models, because it determines the migration direction of the sunspot activity belts (e.g. Krause & Rädler 1980).

References

Belvedere, G., Proctor, M. R. E., Lanzafame, G.: 1991, Nat **350**, 481
Brandenburg, A., Moss, D., Tuominen, I.: 1992, A&A **265**, 328
Busse, F. H., Cuong, P. G.: 1977, Geophys. Astrophys. Fluid Dyn. **8**, 17
Chandrasekhar, S.: 1961, Hydrodynamic and Hydromagnetic Stability. Oxford, Clarendon Press
Durney, B. R.: 1987, In The internal solar angular velocity (ed. B. R. Durney & S. Sofia), Reidel, Dordrecht p.235
Durney, B. R.: 1991, ApJ **378**, 378
Frisch, U., She, Z. S., Sulem, P. L.: 1987, Physica **28D**, 382
Gilman, P. A.: 1977, Geophys. Astrophys. Fluid Dyn. **8**, 93
Gilman, P. A.: 1978, Geophys. Astrophys. Fluid Dyn. **11**, 157
Gilman, P. A., Howard, R.: 1984, Solar Phys. **93**, 171
Glatzmaier, G. A., Gilman, P. A.: 1982, ApJ **256**, 316
Hart, J. E., Glatzmaier, G. A., Toomre, J.: 1986, J. Fluid Mech. **173**, 519
Kitchatinov, L. L.: 1986, Geophys. Astrophys. Fluid Dyn. **35**, 93
Kitchatinov, L. L., Rüdiger, G.: 1993, A&A **276**, 96
Kitchatinov, L. L., Rüdiger, G., Pipin, V. V. 1993 (preprint)
Krause, F., Rädler, K.-H.: 1980, Mean-Field Magnetohydrodynamics and Dynamo Theory. Akademie-Verlag, Berlin
Patera, A.: 1984, J. Comp. Phys. **54**, 468
Pulkkinen, P., Tuominen, I., Brandenburg, A., Nordlund, Å., Stein, R.F.: 1991, In The Sun and cool stars: activity, magnetism, dynamos, IAU Coll. 130 (ed. I. Tuominen, D. Moss & G. Rüdiger), Lecture Notes in Physics, Springer-Verlag p.98

Pulkkinen, P., Tuominen, I., Brandenburg, A., Nordlund, Å., Stein, R. F.: 1993, A&A **267**, 265

Roberts, P. H.: 1968, Phil. Trans. Roy. Soc. **263**, 93

Rüdiger, G.: 1977, Astron. Nachr. **298**, 245

Rüdiger, G.: 1980, Geophys. Astrophys. Fluid Dyn. **16**, 239

Rüdiger, G.: 1989, Differential rotation and Stellar Convection: Sun and solar-type stars. Gordon & Breach, New York

Rüdiger, G., Tuominen, I.: 1990, In Solar Photosphere: Structure, Convection and Magnetic Fields (ed. J. O. Stenflo), Kluwer Acad. Publ., Dordrecht p.315

Schmitt, D.: 1987, A&A **174**, 281

Tuominen, I.: 1990, In The dynamic Sun (ed. Dezsõ), Publ. Debrecen Heliophys. Obs. p.27

Virtanen, H.: 1989, Solar observational hydrodynamics from the sunspot group statistics. Licentiate thesis, Univ. of Helsinki

Ward, F.: 1965, ApJ **141**, 534

Yoshimura, H.: 1975, ApJS **29**, 467

Zhang, K.-K., Busse, F. H.: 1987, Geophys. Astrophys. Fluid Dyn. **39**, 119

Zhang, K.-K.: 1992, J. Fluid Mech. **236**, 535